

# TESTING THE INFLUENCE OF 3D COUPLING EFFECTS ON THE LATERAL RESPONSE OF NON-PLANAR T-SHAPE WOOD FRAME SHEAR WALLS

Diego Valdivieso<sup>1</sup>, Diego Lopez-Garcia<sup>2</sup>, José Luis Almazán<sup>3</sup>, Jairo Montaña<sup>4</sup>,  
Pablo Guindos<sup>5</sup>

**ABSTRACT:** Cumulative shear wall overturning (CSWO) is a common response of structural models of multi-story Light-Frame Timber Buildings (LFTBs) under lateral loads. Governed by holdown uplift and shear wall (SW) bending, large CSWO occurs in LFTBs due to the light self-weight of wood and the dominant rocking flexibility of stiff SWs. Even though CSWO is paramount in seismic design because of its effect on the flexibility of LFTBs (making hard to achieve the inter-story drift limits), this phenomenon is not incorporated into the structural models of LFTBs. For instance, in the design of LFTBs for lateral loads it is assumed that SWs behave as planar isolated elements. However, CSWO may be influenced by 3D coupling effects (3D-SWCE) in non-planar SWs such as T or L assemblies. This paper describes a large full-scale experiment of a 7.32 m x 5.1 m assembly, performed to gather insight into 3D-SWCEs through the cyclic evaluation of a non-planar T-shape SW. Results showed an asymmetric behaviour of the T-shape SW with increments of 20% and 98% in elastic stiffness and maximum capacity, respectively, with respect to those of a planar SW. It is concluded that 3D-SWCEs have a significant structural influence on the response of LFTBs.

**KEYWORDS:** Wood frame construction, light-frame shear walls, non-planar, T-shape, 3D-SWCE.

## 1 INTRODUCTION

Light frame timber building (LFTB) is one of the alternatives evaluated by the Chilean construction industry to eventually replace concrete and steel mid-rise buildings, reducing the housing deficit and the contribution of the construction industry to the global greenhouse gas emissions [1].

A LFTB is the result of the assembly of several components with repetitive members such as walls, floors, and roof systems connected by intercomponent connections forming a three-dimensional highly indeterminate structural system. Then, gross simplifying assumptions are made (e.g., walls assumed as in-plane resistant components) for its design and analysis [2]. When LFTBs are subjected to earthquake loads, cumulative rotation effects are presented when the shear walls are assumed to behave as isolated cantilever components due to the hold-down elongation and bending deformation of the wall [3]. However, full-scale test

results [4-8] showed that current mechanical models [3,9,10] suffer from several limitations as the system effects are not captured. In this paper system effect refers to the interaction between the components of a building (i.e., shear walls, floor, or roof systems) which modifies the response of isolated components. It is then important to experimentally evaluate the mechanism that controls the system effect considering component-level specimens, as the experimental campaigns in light-frame structures that identified the system effect had been done based on building-level specimens [4-8].

### 1.1 NON-PLANAR TIMBER SHEAR WALLS

For mid-rise buildings in highly seismic-prone areas, such as Chile, wood-frame shear walls usually adopt a strong structural configuration (i.e., strong shear wall or SSW), consisting of 41 × 185 mm (2×8) framing members, sturdy end studs (typically comprising 4 or more members), strong hold-down, wood structural panel (WSP) - typically OSB on both sides-, and closely spaced

<sup>1</sup> Diego Valdivieso, Pontificia Universidad Católica de Chile, Centro Nacional de Excelencia para la Industria de la Madera (CENAMAD) & Centro de Innovación en Madera (CIM UC-CORMA, Chile, [dvaldivieso@uc.cl](mailto:dvaldivieso@uc.cl))

<sup>2</sup> Diego Lopez-Garcia, Pontificia Universidad Católica de Chile & Research Center for Integrated Disaster Risk Management (CIGIDEN) ANID FONDAP 1522A0005, Chile, [dlg@ing.puc.cl](mailto:dlg@ing.puc.cl)

<sup>3</sup> José Luis Almazán, Pontificia Universidad Católica de Chile, Centro Nacional de Excelencia para la Industria de la Madera (CENAMAD) & Centro de Innovación en Madera (CIM UC-CORMA, Chile, [jlalmaz@ing.puc.cl](mailto:jlalmaz@ing.puc.cl))

<sup>4</sup> Jairo Montaña, Centro Nacional de Excelencia para la Industria de la Madera (CENAMAD) and Centro de Innovación en Madera (CIM UC-CORMA), Chile, [jamontano@uc.cl](mailto:jamontano@uc.cl)

<sup>5</sup> Pablo Guindos, Pontificia Universidad Católica de Chile, Centro Nacional de Excelencia para la Industria de la Madera (CENAMAD) & Centro de Innovación en Madera (CIM UC-CORMA, Chile, [pguindos@ing.puc.cl](mailto:pguindos@ing.puc.cl))

edge and field nailing patterns [11-13]. In the layout of a building, SSWs are typically assembled in T-shape, L-shape, and/or U-shape non-planar SSWs based on the architectural project. These non-planar shear walls have been deeply studied in concrete structures [14, 15], identifying coupling effects (i.e., the effect of transverse shear walls on the in-plane response of a wall) that need to be addressed in SSWs. In this paper, the coupling effect presented in non-planar SSWs is denoted 3D shear wall coupling effect (3D-SWCE).

In light-frame timber structures, 3D-SWCE has been identified as one of the key factors to be evaluated for a better understanding of LFTBs [16]. The 3D-SWCE has been evaluated experimentally in conventional shear walls [17, 18] (i.e., the term conventional shear wall was introduced in [11] for referring to wood frame shear wall consisting of a 1.2–2.4 m long wood frame with 38 × 89 mm (2×4) interior studs spaced at 400 mm on center, double end studs, single members for the top and sole plate, and discrete hold-downs to prevent overturning of the wall) and partitional walls [19, 20] as an alternative for replacing the installation of hold-downs. Experimental results showed that transverse shear walls have the potential to increase the racking stiffness of a wall to the point where no hold-down is needed. An analytical procedure was introduced in [21] for computing the tying-down effect of transverse walls on the load-carrying capacity of partially anchored conventional shear walls. The procedure demonstrates that transverse shear walls have the potential to increase the lateral in-plane load-carrying capacity of a shear wall. That increment reduces as the aspect ratio of the wall reduces as well (i.e., up to 100% of increment in lateral load for shear walls with a 1:2 aspect ratio, from up to 32% for walls with a 1:0.5 aspect ratio). Even though this procedure is a starting point for the evaluation of 3D-SWCE, it considers only the effect of transverse shear walls by their uplift strength/stiffness, neglecting the out-of-plane strength/stiffness component. Further experimental evaluation is needed in the case where SSWs are used (i.e., as the in-plane/out-of-plane stiffness and strength are higher in SSWs than in conventional shear walls). To the best of the authors' knowledge, no previously published studies have described the cyclic behavior of non-planar SSWs.

The 3D-SWCE has been studied in cross-laminated timber (CLT) shear walls experimentally and numerically [22, 23]. The effect of the out-of-plane walls on the in-plane strength and stiffness of an I-shape CLT non-planar shear wall was reported in [22]. A positive influence on the initial lateral stiffness (i.e., increment of up to 155%) and peak strength (i.e., increment of up to 60%) was found because of the added out-of-plane walls with respect to an isolated wall assembly. Furthermore, the 3D-SWCE seems not to affect the failure mechanism and deformation capacity of the system. The study highlights that a key component for achieving 3D-SWCE is a properly detailed connection between transverse and in-plane walls in order to use them as an uplift restraint system.

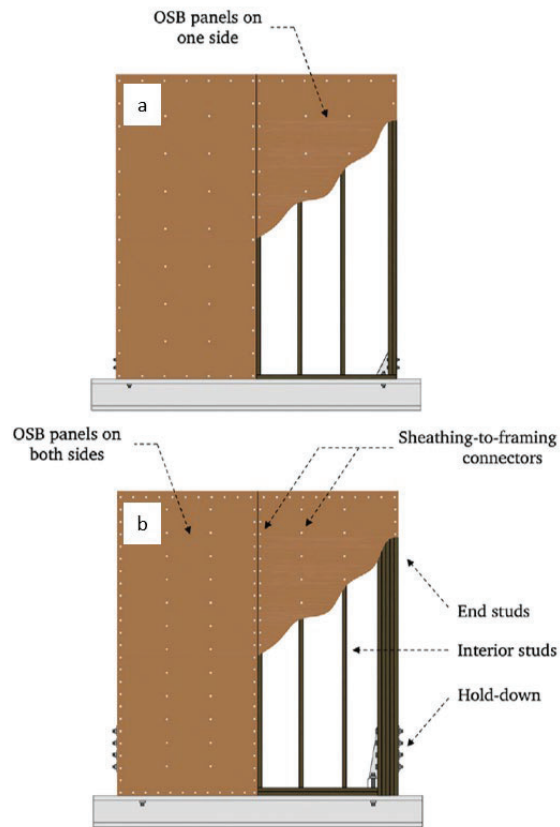


**Figure 1:** Schematic configuration of (a) conventional and (b) strong wood frame shear wall. Taken from [11]

## 2 SCOPE

This investigation aims at evaluating experimentally the lateral cyclic response of a non-planar T-shape wood frame strong shear wall as a way to represent part of the system effects found in LFTBs. Also, as previous studies identified that the wall-to-wall perpendicular connections are crucial for achieving 3D-SWCEs, two alternatives were evaluated experimentally.

## 3 METHODOLOGY

Connection-level and assembly-level tests were carried out under monotonic and/or cyclic loading according to ASTM E564-06 [5] and ASTM E2126-19 [6], respectively. The loading protocol was displacement-controlled and applied until failure of the specimen.

### 3.1 CONNECTION-LEVEL TEST

Two different configurations of wall-to-wall perpendicular connections were assembled. Both connections (i.e., screwed and slotted) were selected to facilitate wall installation considering off-site construction techniques. The connection-level specimens are representative of an end-stud-to-end-stud perpendicular connection (i.e., for a wall-to-wall perpendicular connection, end-studs are connected). Specimens consider two lateral elements and one central element manufactured with 41 mm x 135 mm (2x6)

dimensional Chilean radiata pine (RP) lumber mechanically graded as C16 according to NCh1198 [26]. As SSWs are sheathed with OSB, a layer of OSB is attached at both sides of the central element. Screwed connection considers two pairs per shear plane of four crossed screws in an X-position installed at 45°. Slotted connections consider one slot connector per shear plane. Details of each specimen are summarized in Table 1. Each configuration consists of 3 specimens: 1 for monotonic testing, and 2 for cyclic testing.

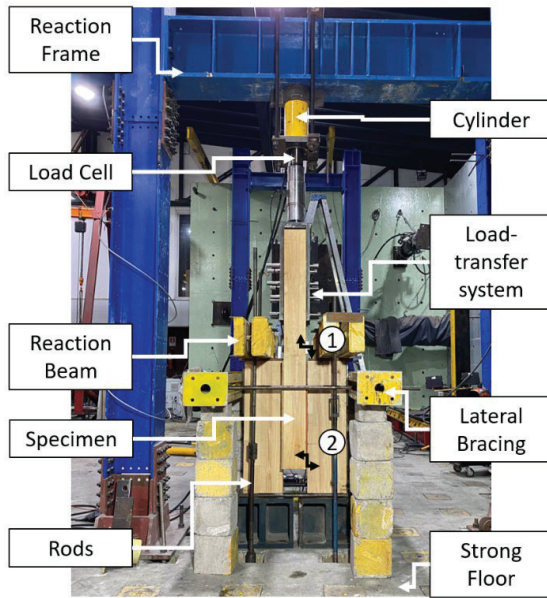


Figure 2: Connection-level test setup

A reaction steel frame was used to perform the connection-level tests. As shown in Figure 2, the reaction steel frame is anchored to a strong floor. Two heavy-duty steel beams are installed at each side of the specimen reacting against the strong floor through four high-strength rods (Figure 2). The load was applied by a double-action cylinder of +/- 588 kN and +/- 75 mm of force and displacement capacity, respectively, which transfers the vertical load to the specimen through a load-transfer system that consists of two steel plates attached to the specimen through bolts. As shown in Figure 2, all specimens were instrumented with four (i.e., two per shear plane) displacement transducers (LVDTs) for measuring the slip of the connection (labelled as 1 in Figure 2), two (i.e., one per shear plane) LVDTs for monitoring the rotation of the lateral end-studs (labelled as 2 in Figure 2) and one double-effect load cell to capture the shear force between end-studs.

Table 1: Connection-level specimen details

Connection Type	Lateral Element <sup>b</sup>	Central Element <sup>b</sup>	Fast.or Conn. Type
45XSc <sup>a</sup>	(4)41x135	(10)41x135	ESCRFTZ 8.0X300 <sup>c</sup>
Slot90	(6)41x135	(12)41x135	SLOT90 <sup>d</sup>

Notes:

- Screw is abbreviated as Sc
- For assembling each element, wood-frames are glued together following NCh2150 [27] prescriptions.
- ESCRFTZ 8.0X300 per ETA-13/0796 of 12/15/2017 manufactured by Simpson Strong-Tie.
- SLOT 90 per ETA-19/0167 of 04/05/2019 manufactured by Rothoblaas.

### 3.2 ASSEMBLY-LEVEL TEST

Specimens used for the planar and non-planar T-shape walls are representative of typical ground-level walls of a 7-story building designed per the Chilean seismic design code NCh433 [28]. Details of the wall specimens are summarized in Table 2. Double plates at the top and bottom of the wall were nailed to the studs with  $\phi 3.0$  mm x 80 mm smooth shank nails that conform to ASTM F1667 [29]. All framing elements were 41 mm x 185 mm (2x8) C16 Chilean RP dimensional lumber, with a nominal modulus of elasticity  $E = 7900$  MPa according to NCh1198 [26]. The walls were sheathed on both sides with 11.1 mm thick APA-rated OSB panels [30] with  $G = 1307.5$  MPa (measured in previous studies [11]), and pneumatically driven to the frame with  $\phi 2.9$  mm x 80 mm spiral nails. OSB sheathing layers were installed at both sides of the specimens and attached to the lower top plate and to the upper bottom plate as illustrated in Figure 3. According to the SDPWS [31], edge-nailing at the end studs should be uniformly distributed among the four framing members and spaced at a maximum of 300 mm. In order to transfer the lateral load to each specimen, a built-up collector beam of 205 mm x 207 mm (i.e., five members of 41 mm x 185 mm C16 RP plus an 11.1 mm thick OSB layer on top and bottom) was mechanically attached to the top plate through 38 Simpson Strong-Tie's SCDP221100 screws. For assembling the non-planar T-shape SSW, one type A (i.e., for the web) wall and two type B (i.e., for the flange) wall were used. For the wall-to-wall perpendicular connection (i.e., for attaching each flange to the web of the T-shape wall), six SLOT90 connector are used. The connectors are installed into the walls and fixed using two (i.e., one screw for wall) Simpson Strong-Tie's SDCF22614 screws (Figure 3). The planar SSW is a type C wall.

Table 2: Wall type configuration

Wall Type <sup>n</sup>	Wall size (L by H)	Wood Structural Panel (WSP)		
		Thickness	Sheathing Nails <sup>d</sup>	Spacing edge/field
A <sup>a,c</sup>	1 2440x2481	11.1	$\phi 2.9 \times 80$	100/200
B <sup>b,c</sup>	2 2440x2481	11.1	$\phi 2.9 \times 80$	100/200
C <sup>b,c</sup>	1 2440x2481	11.1	$\phi 2.9 \times 80$	100/200

Notes:

- Wall framing consisted of 41mm x 185 mm (2x8) C16 Chilean RP [26] studs at 400mm o.c., (2) 41mm x 185 mm used as a central stud, (4) 41mm x 185 mm studs mechanically joined and located symmetrically with respect to the rod and (5) 41mm x 185 mm studs mechanically joined are used as end-studs.
- Wall framing consisted of 41mm x 185 mm (2x8) C16 Chilean RP [26] studs at 400mm o.c., (2) 41mm x 185 mm used as a central stud, (4) 41mm x 185 mm studs mechanically joined

and located symmetrically with respect to the rod are used as end-studs.

c) Wall shear anchorage consisted of  $\phi 32$  mm x 220 mm ASTM A193 Grade B7 anchor bolts (14 and 15 for wall type A and B, respectively) with  $\phi 80$  mm x 4.0 mm Grade A36 washers. Overturning restraint provided by  $\phi 38.1$  mm ASTM A193 Grade B7 rods with 31.75 mm thick bearing plate (i.e., Simpson Strong-Tie PL16-5x12), a take-up device (i.e., Simpson Strong-Tie ATUD14), a 9.5 mm thick bearing plate (i.e., Simpson Strong-Tie BP 1-1/2), and ASTM A563 Grade DH double hexagonal nut.

d) nails installed considering a minimum of 20/40 mm of end/edge distance, respectively. According to EN14592:2008+A1:2012 [32].

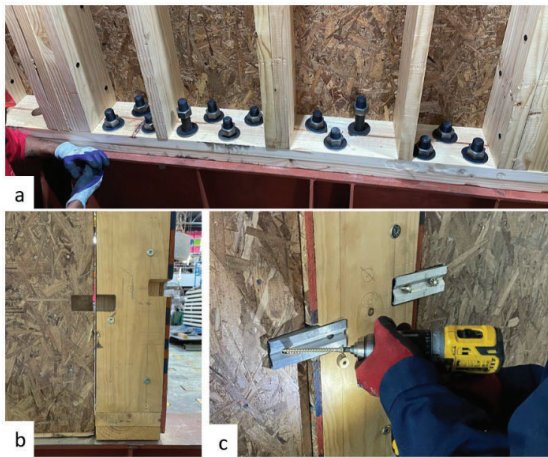


**Figure 3:** (a) sliding restrain system for wall type A and B, and, wall-to-wall connection detail; (b) slot disposition; and (c) installation of the SLOT90 connector

An L-shape cantilever reaction wall, a strong floor, and a T-shape reaction steel beam were used to perform the assembly-level tests following ASTM E2126-19 [25] prescriptions (Figure 4). As shown in Figure 3, the specimens were attached to the reaction beam through 43  $\phi 32$  mm x 220 mm ASTM A193 Grade B7 anchor bolts to prevent sliding in the T-shape SSW. In order to prevent sliding and to measure the shear force during the cyclic test in the planar SSW, a couple of cylinders reacting against a L-shape connector were installed at each side of the wall (element 9 in Figures 5 and 6). The walls continuous rod system reacts against the top flange of the reaction beam through a system of double hexagonal nuts. Out-of-plane support was provided to the 2D SSW in such a way that in-plane displacements were not affected. In order to capture the 3D response of the T-shape non-planar shear wall, a bidirectional cyclic test was performed according to FEMA 461 [33]. The hexagonal protocol from FEMA 461 [33] consider as a base the test protocol per ASTM E2126-19 [25] method C where a 100% and 50% of the target displacement were applied in the longitudinal and transverse direction. The lateral load was applied by a hydraulic bidirectional actuator of +588 kN/-294kN and +/- 200 mm of force and displacement capacity, respectively, in the longitudinal direction, and by a hydraulic bidirectional actuator of +588 kN/-294kN and +/- 50 mm of force and displacement capacity, respectively, in the transverse direction. Both actuators

transfer the lateral load to the specimen through the collector beam. The T-shape non-planar SSW and the planar SSW are connected by a steel pinned-beam, allowing the in-plane loading transferring and decoupling the racking response of the specimens (Figure 4).

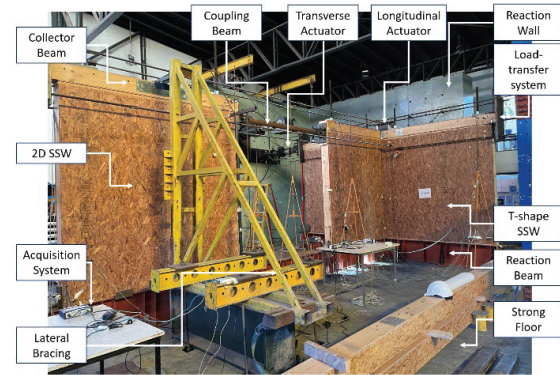


**Figure 4:** Assembly-level test setup

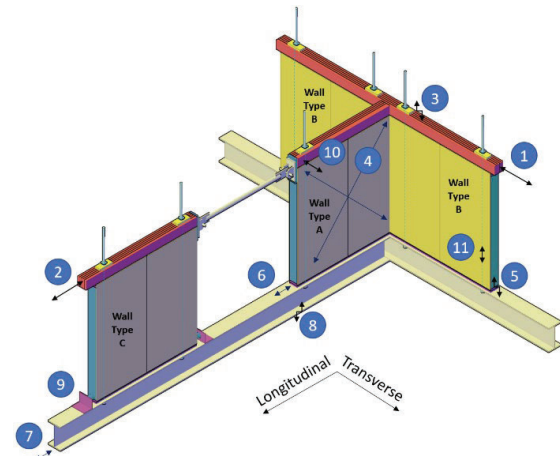


**Figure 5:** Assembly-level specimen and instrumentation detail

The specimen were instrumented with 41 displacement transducers (LVDTs), two cell load at the reaction cylinders (element 9 in Figures 5 and 6), and two load cell and displacement transducers (LVDT) incorporated into the actuator to capture the lateral displacement and shear force along each axis of the specimens (elements 1 and 2 in Figure 5), the slip of the wall with respect to the steel reaction beam (elements 6 and 8 in Figures 5 and 6), the diagonal (shear) deformation (element 4 in Figures 5 and 6), uplift in the exterior edge of the wall (element 5 in Figures 5 and 6), the out-of-plane displacement of the T-shape SSW web (element 10 in Figures 5 and 6), the relative displacement of the steel reaction beam with respect to the strong floor (element 7 in Figure 5), and the compressive deformation under the bearing plate of the strong-rod system (element 3 in Figures 5 and 6). To measure the tension in the rods of the continuous hold-down, seven unidirectional strain-gauges were attached to the rods (element 11 in Figures 5 and 6).

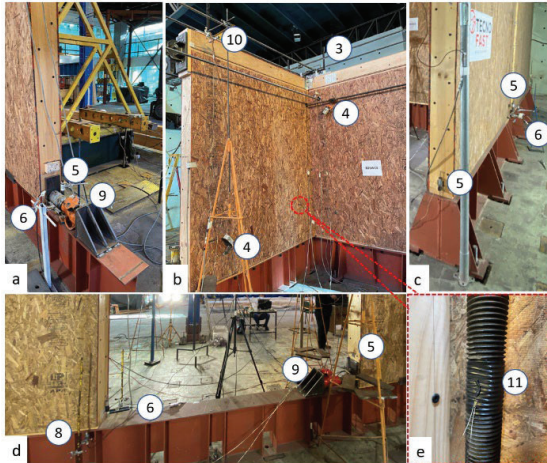


**Figure 6:** Test setup: (a) sliding restraint system for the 2D SSW; (b) T-shape SSW instrumentation detail; (c) transverse view of the T-shape SSW; (d) detail of the instrumentation at the wall corners; and (e) strain gauge installation in a rod.

## 4 RESULTS

Failure mode, hysteresis shape, and six engineering parameters were established for connection-level and assembly-level test results: (1) elastic stiffness ( $K_e$ ), calculated as the secant stiffness between zero and 40% of maximum load  $F_{max}$ ; (2) yield displacement ( $\Delta_y$ ); (3) yield force ( $F_y$ ); (4) ultimate displacement ( $\Delta_u$ ), defined as the displacement after post-peak load where the load dropped to  $F_u = 0.8 F_{max}$ ; (5) ultimate force ( $F_u$ ); and, (6) ductility ( $\mu$ ), defined as the ratio of  $\Delta_u$  to  $\Delta_y$ . Moreover, the lateral behavior of the T-shape SSW is compared with that of the 2D SSW used in this study as reference.

### 4.1 CONNECTION-LEVEL TESTS

The slotted connection (i.e., connection type Slot90) shows two failure modes: (i) compression parallel to the grain crushing at the wood studs; and (ii) local yielding in the SLOT90 connector. The screwed connection (i.e., connection type 45XSc) shows two failure modes: (i) excessive bend in the screws, wood crushing and tearing in OSB sheathing layer; (ii) withdrawal failure of at least one screw of the group; (iii) pull-through of the screws head; and (iv) tension failure of at least one screw of the group. Note that in failure modes (ii) to (iv) pulling out of the connected wood members was present.

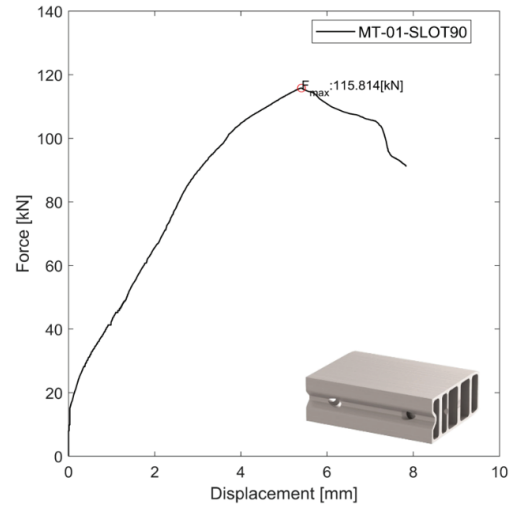


**Figure 7:** Monotonic test results of Slot90 wall-to-wall perpendicular connections.

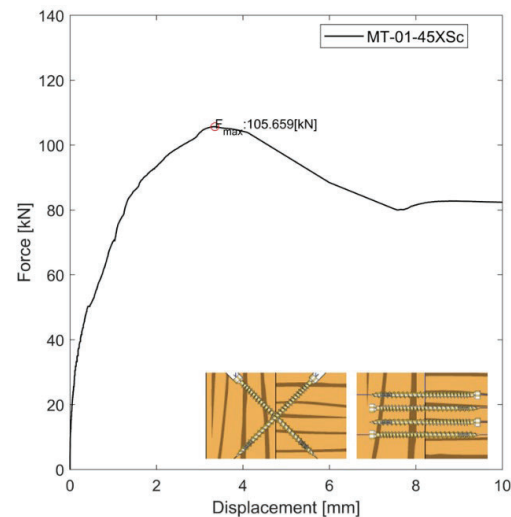


**Figure 8:** Monotonic test results of 45XSc wall-to-wall perpendicular connections

Monotonic results for each connection-level test are shown in Figures 7 and 8, in which the reported displacement is the differential slip between the wood frames, and the force is that taken by only one SLOT90 or group of four inclined ESCRFTZ 8.0X300 screws along a single shear plane. Based on monotonic test results, engineering parameters are summarized in Table 3. Both connections showed almost the same peak load and higher elastic stiffness which is attributable to the wood parallel to the grain stiffness/strength and axial stiffness of fully threaded screws for the case of connection type Slot90 and 45XSc, respectively. From a ductility point of view, connection type 45XSc showed almost four times higher values than the Slot90 connection. However, this tendency was not evidenced in cyclic test results were the 45XSc and Slot90 connection types show almost the same deformation capacity (Figures 9 and 10). Finally, based on preliminary numerical models, for achieving 3D-SWCE in a T-shape non-planar SSW the wall-to-wall

perpendicular connection needs to have a stiffness equal to 40% of that of the 2D SSW. When 3D-SWCE is achieved, the numerical model predicted a 20% reduction in the lateral displacement of a 1-story SSW. Based on previous evaluation, both connection types are good candidates as wall-to-wall perpendicular connections.

**Table 3:** Engineering parameters from monotonic connection-level test results

Connection Type	$K_c$ kN/mm	$\Delta_y$ mm	$F_y$ kN	$\Delta_u$ mm	$F_u$ kN	$\mu$
45XSc	156.0	0.59	92.4	6.74	84.5	11.4
Slot	39.2	2.64	103.6	7.72	92.65	2.9

The cyclic force-displacement test response for both connection types is presented in Figures 9 and 10. Again, results are expressed in terms of differential slip per connector or group of fasteners per shear plane. Cyclic test results for all tested connections depict a strong pinching effect due to the wood frame crushing at the shear planes. Moreover, strength and stiffness degradation after repeated cycles were found in all tests. In particular, in the 45XSc connection type, an abrupt reduction of the stiffness and strength was found after reaching the peak load as the withdrawal failure tends to be more brittle than the parallel to the grain crushing evidenced in the Slot90 connection.

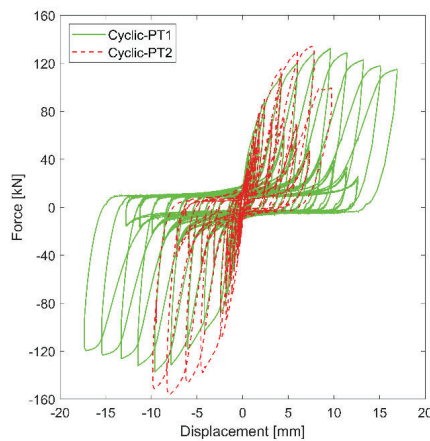


**Figure 9:** Cyclic test results of Slot90 wall-to-wall perpendicular connections.

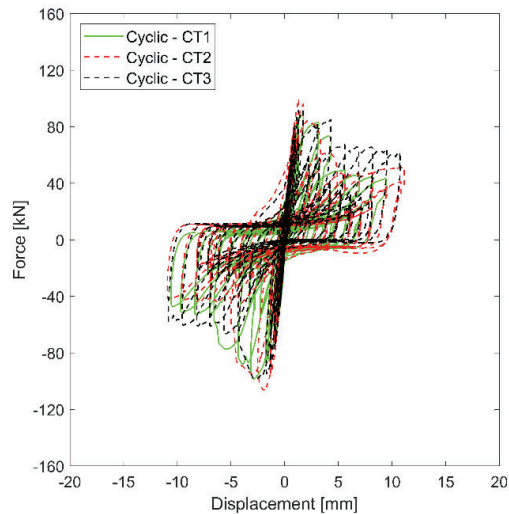


**Figure 10:** Cyclic test results of 45XSc wall-to-wall perpendicular connections.

## 4.2 ASSEMBLY-LEVEL TESTS

A comparison between the backbone curves obtained from bidirectional cyclic loading on the assembly-level full-scale tests is presented in Figure 11. Based on backbone curves results, engineering parameters are summarized in Table 4. Assembly-level tests showed an asymmetric behaviour of the T-shape SSW with increments of up to 19% and 98% in the elastic stiffness and maximum capacity, respectively, compared to those of a 2D SSW. However, a mean reduction of 44% in ductility was also observed.

The hysteretic curves of the T-shape SSW and the control wall (i.e., 2D SSW) are shown in Figures 12 and 13, respectively. The reported displacement is the effective displacement of the wall measured at the collector axis where the actuator was located (i.e., longitudinal collector). The effective displacement is the measured lateral displacement of the wall minus the displacement measured at the specimen-to-reaction beam relative to the reaction beam-to-strong floor. The overall shape of the 2D SSW hysteretic loops was consistent with that reported in previous research [12, 13]. However, the T-shape SSW cyclic response was asymmetric (i.e., 44% difference in peak strength) with a faster degradation of strength and stiffness in the flange side of the specimen (i.e., the negative branch of the cyclic response in Figure 13), which is attributable to the premature detachment of the OSB sheathing (i.e., nailed OSB-to-wood frame connection failure) close to the flange of the wall. The 2D SSW and the T-shape SSW specimens showed elastic response up to a drift of about 0.6% and 0.8%, respectively, and then a nonlinear response was observed, attributable to the nailed OSB-to-wood frame connections. After the specimens reached the peak strength, progressive strength and stiffness degradation was found. As expected, high redundancy was evident in the specimens because of the nailed connections, resulting in high drift levels with no brittle failures. Hence, as the

lateral behavior of the specimens was governed by the nailed connection response, the hysteresis was markedly pinched because of the non-reversible crushing effect of the nails.

**Table 4:** Engineering parameters from cyclic backbone curves of the assembly-level test results

Wall Conf.	$K_e$ kN/mm	$\Delta_y$ mm	$F_y$ kN	$\Delta_u$ mm	$F_u$ kN	$\mu$
T-shape SSW+	4.04	18.9	76.3	68.6	67.3	3.6
T-shape SSW-	4.83	22.7	109.4	64.3	104.2	2.9
<b>T-shape SSW<sub>mean</sub></b>	<b>4.44</b>	<b>20.8</b>	<b>92.9</b>	<b>66.5</b>	<b>85.8</b>	<b>3.3</b>
2D-SSW+	3.58	17.1	61.3	88.1	55.3	5.1
2D-SSW-	4.06	13.8	55.9	92.4	52.6	6.7
<b>2D- SSW<sub>mean</sub></b>	<b>3.82</b>	<b>15.4</b>	<b>58.6</b>	<b>90.2</b>	<b>54.0</b>	<b>5.9</b>

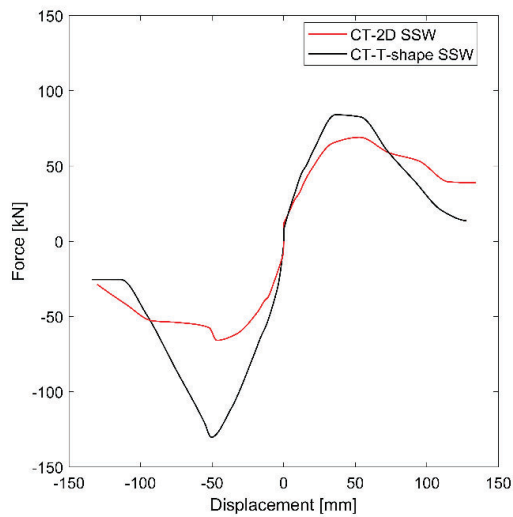


**Figure 11:** Comparison between the backbone curves of in-plane response of the T-shape SSW (black) and the 2D SSW (red).

## 5 CONCLUSIONS

Findings of this research reinforce the idea of taking advantage of the 3D-SWCE on the lateral response of LFTBs. The ultimate objective is to achieve a cost-effective structural design and to better understand CSWO, so that traditional pseudo-3D design practices be discouraged. The next steps of this research program include the calibration of analytical and numerical models for non-planar timber shear walls. Further research is needed to elucidate potential 3D effects on other non-planar walls such as U- or L-shape assemblies.

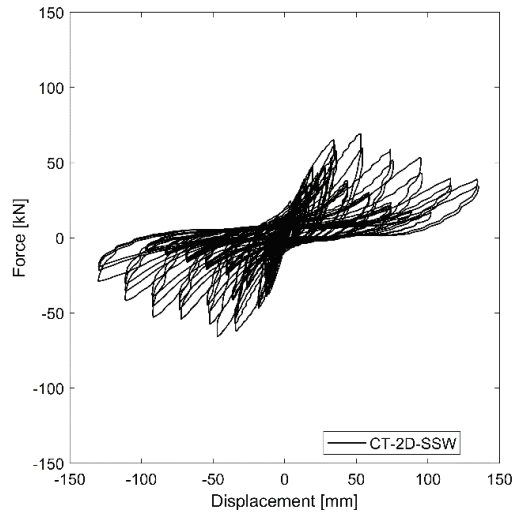


**Figure 12:** In-plane cyclic response of the 2D SSW.

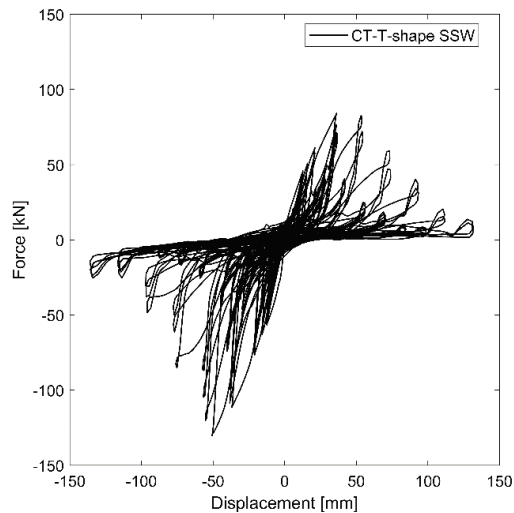


**Figure 13:** In-plane cyclic response of the 2D SSW

## ACKNOWLEDGEMENTS

Financial support was provided by CONICYT (Doctorado Nacional 2018–21180074), by VRI-UC, by ANID BASAL FB210015 (CENAMAD), and by the Research Center for Integrated Disaster Risk Management (CIGIDEN) ANID FONDAP 1522A0005.

## REFERENCES

- [1] Almeida De Araujo, V., Cortez-Barbosa, J., Garcia, J. N., Gava, M., Laroca, C., & César, S. F. (2016). Woodframe: viviendas de entramado ligero para países en desarrollo. *Revista de la Construcción*, 15(2), 78-87.
- [2] Hopkins, A. K., Fell, B. V., Deierlein, G. G., & Miranda, E. (2014). Large-scale tests of seismically enhanced planar walls for residential construction.

- Report No. 186, John A. Blume Earthquake Engineering Center, Stanford, USA.
- [3] Leung, T., Asiz, A., Chui, Y., Hu, L. J., & Mohammad, M. (2010). Predicting lateral deflection and fundamental natural period of multi-storey wood frame buildings. *11<sup>th</sup> World Conference on Timber Engineering*, Trentino, Italy.
- [4] Van de Lindt, J. W., Pei, S., Pryor, S. E., Shimizu, H., & Isoda, H. (2010). Experimental seismic response of a full-scale six-story light-frame wood building. *Journal of Structural Engineering*, 136(10), 1262-1272.
- [5] Collins, M., Kasal, B., Paevere, P., & Foliente, G. C. (2005). Three-dimensional model of light frame wood buildings. II: Experimental investigation and validation of analytical model. *Journal of Structural Engineering*, 131(4), 684-692.
- [6] Winkel, M., & Smith, I. (2010). Structural behavior of wood light-frame wall segments subjected to in-plane and out-of-plane forces. *Journal of Structural Engineering*, 136(7), 826-836.
- [7] Paevere, P. J. (2002). Full-scale testing, modelling and analysis of light-frame structures under lateral loading. *Ph.D. Thesis*, University of Melbourne, Melbourne, Australia.
- [8] Tomasi, R., Sartori, T., Casagrande, D., & Piazza, M. (2015). Shaking table testing of a full-scale prefabricated three-story timber-frame building. *Journal of Earthquake Engineering*, 19(3), 505-534.
- [9] Pei, S., & Van de Lindt, J. W. (2011). Seismic numerical modeling of a six-story light-frame wood building: comparison with experiments. *Journal of Earthquake Engineering*, 15(6), 924-941.
- [10] Pang, W., Ziaei, E., & Filiatrault, A. (2012). A 3D model for collapse analysis of soft-story light-frame wood buildings. *World Conference on Timber Engineering*, Auckland, New Zealand.
- [11] Estrella, X., Guindos, P., Almazán, J. L., & Malek, S. (2020). Efficient nonlinear modeling of strong wood frame shear walls for mid-rise buildings. *Engineering Structures*, 215, 110670.
- [12] Estrella, X., Malek, S., Almazán, J. L., Guindos, P., & Santa María, H. (2021). Experimental study of the effects of continuous rod hold-down anchorages on the cyclic response of wood frame shear walls. *Engineering Structures*, 230, 111641.
- [13] Guíñez, F., Santa María, H., & Almazán, J. L. (2019). Monotonic and cyclic behaviour of wood frame shear walls for mid-height timber buildings. *Engineering Structures*, 189, 100-110.
- [14] Kolozvari, K., Kalbasi, K., Orakcal, K., & Wallace, J. (2021). Three-dimensional shear-flexure interaction model for analysis of non-planar reinforced concrete walls. *Journal of Building Engineering*, 44, 102946.
- [15] Ramos, L., & Hube, M. (2020). Contribution of coupling elements to the seismic demand of walls in reinforced concrete buildings. *Latin American Journal of Solids and Structures*, 17(2), e256.
- [16] Seible, F., Filiatrault, A., & Uang, C. M. (1999). Proceedings of the Invitational Workshop on Seismic Testing, Analysis and Design of Woodframe Construction. *CUREE Publication No. W-01*, Consortium of Universities for Research in Earthquake Engineering, Richmond, USA.
- [17] Suzuki, S. (1990). Effect of cross-walls on lateral stiffness of light-frame buildings. *International Timber Engineering Conference*, Tokyo, Japan.
- [18] Sugiyama, H., & Isono, R. (1983). The effect of perpendicularly arranged wall on the shear strength of plywood sheathed wall. *1983 Annual Meeting*, Architectural Institute of Japan, Tokyo, Japan.
- [19] NAHB Research Center, Inc. (2001). *Wood Shear Walls with Corners*. Partnership for Advanced Technology in Housing, Washington, USA.
- [20] Dolan, J. D., & Heine, C. P. (1997). Sequential phased displacement tests of wood-framed shear walls with corners. *Report No. TE-1997-003*, Virginia Polytechnic Institute and State University, Blacksburg, USA.
- [21] Girhammar, U. A., & Källsner, B. (2008). Effect of transverse walls on capacity of wood-framed wall diaphragms without tie-downs. *10<sup>th</sup> World Conference on Timber Engineering*, Miyazaki, Japan.
- [22] Stoner, M. W. (2020). Performance of cross-laminated timber as a residential building material subject to tornado events. *Ph.D. Thesis*, Clemson University, Clemson, USA.
- [23] Ruggeri, E., D'Arenzo, G., Fossetti, M., & Seim, W. (2022). Investigating the effect of perpendicular walls on the lateral behaviour of cross-laminated timber shear walls. *Structures*, 46, 1679-1695.
- [24] ASTM (2006). *Standard Practice for Static Load Test for Shear Resistance of Framed Walls for Buildings ASTM E564-06*. ASTM International, West Conshohocken, USA.
- [25] ASTM (2019). *Standard Test Methods for Cyclic (Reversed) Load Test for Shear Resistance of Vertical Elements of the Lateral Force Resisting Systems for Buildings ASTM E2126-19*. ASTM International, West Conshohocken, USA.
- [26] INN (2014). *Madera - Construcciones en Madera - Cálculo NCh 1198*. Instituto Nacional de Normalización, Santiago, Chile. (in Spanish)
- [27] INN (2022). *Madera Laminada Encolada - Clasificación Mecánica y Visual de Madera Aserrada de Pino Radiata NCh 2150*. Instituto Nacional de Normalización, Santiago, Chile. (in Spanish)
- [28] INN (2009). *Diseño Sísmico de Edificios NCh 433 Of1996 Mod. 2009*. Instituto Nacional de Normalización, Santiago, Chile. (in Spanish)
- [29] ASTM (2021). *Standard Specification for Driven Fasteners: Nails, Spikes, and Staples ASTM F1667*. ASTM International, West Conshohocken, USA.
- [30] APA (2012). *Panel Design Specification*. APA - The Engineering Wood Association, Tacoma, USA.
- [31] AWC (2021). *Special Design Provisions for Wind and Seismic ANSI/AWC SDPWS-2021*. American Wood Council, Leesburg, USA.
- [32] BSI (2008). *BS EN 14592: 2008+ A1: 2012 Timber Structures - Dowel-type Fasteners - Requirements*. British Standard Institution, London, UK.

[33]ATC (2007). *Interim Testing Protocols for Determining the Seismic Performance Characteristics of Structural and Nonstructural Components FEMA 461*. Federal Emergency Management Agency, Washington, USA.